



Twisting strategy applied to *N,N*-diorganoquinacridones leads to organic chromophores exhibiting efficient solid-state fluorescence

Masaki Shimizu^{*}, Yuiga Asai, Youhei Takeda, Akinori Yamatani, Tamejiro Hiyama[†]

Department of Material Chemistry, Graduate School of Engineering, Kyoto University, Kyoto University Katsura, Nishikyo-ku, Kyoto 615-8510, Japan

ARTICLE INFO

Article history:

Received 20 April 2011

Revised 16 May 2011

Accepted 18 May 2011

Available online 25 May 2011

Keywords:

Charge transfer

Diaroylbenzenes

Fluorescence

Solid-state emission

Terephthalates

ABSTRACT

A new molecular design of organic emitters exhibiting efficient solid-state fluorescence, which involves planarity breaking of *N,N*-diorganoquinacridones, is presented. The new design principle led to the development of dimethyl 2,5-diaminoterephthalates and 2,5-diamino-1,4-diaroylbenzenes, which emitted green to yellow and yellow to red light with high-to-excellent quantum yields, respectively. In addition, the photoluminescence properties of the diaroylbenzenes were dependent on the morphology and reversibly variable by thermal and solvent vapor stimuli.

© 2011 Elsevier Ltd. All rights reserved.

Organic chromophores that exhibit fluorescence in the visible region with high efficiency in the solid-state have attracted increasing attention in the field of functional materials. This is because the highly efficient solid-state emissions of organic fluorophores are essential for the advances needed to realize optoelectronic devices, such as organic light-emitting diodes (OLEDs),¹ light-emitting field-effect transistors,² semiconductor lasers,³ and fluorescent solid sensors.⁴ However, most organic fluorophores are nonluminescent or only faintly emissive in the solid-state due to concentration quenching induced by molecular aggregation, which is an inherent characteristic of organic solids. Hence, the molecular design and development of organic fluorophores exhibiting highly efficient solid-state emissions have met limited success,⁵ but such fluorophores are of great importance with respect to both practical applications in optoelectronic devices and fundamental studies in solid-state molecular engineering. The reported molecular designs that render fluorophores efficiently luminescent in the solid-state involves (1) the incorporation of a spiro framework; (2) the introduction of bulky substituents; (3) vicinal disubstitution of aryl/aryl or alkenyl/aryl groups on an aromatic ring or alkenyl moiety, and (4) the installation of electron-donating and -withdrawing groups at the molecular ends and/or middles.^{5a} Recently, self-assembly-induced and exciplex-mediated emission enhancement of organic gels is also demonstrated.^{5b–e}

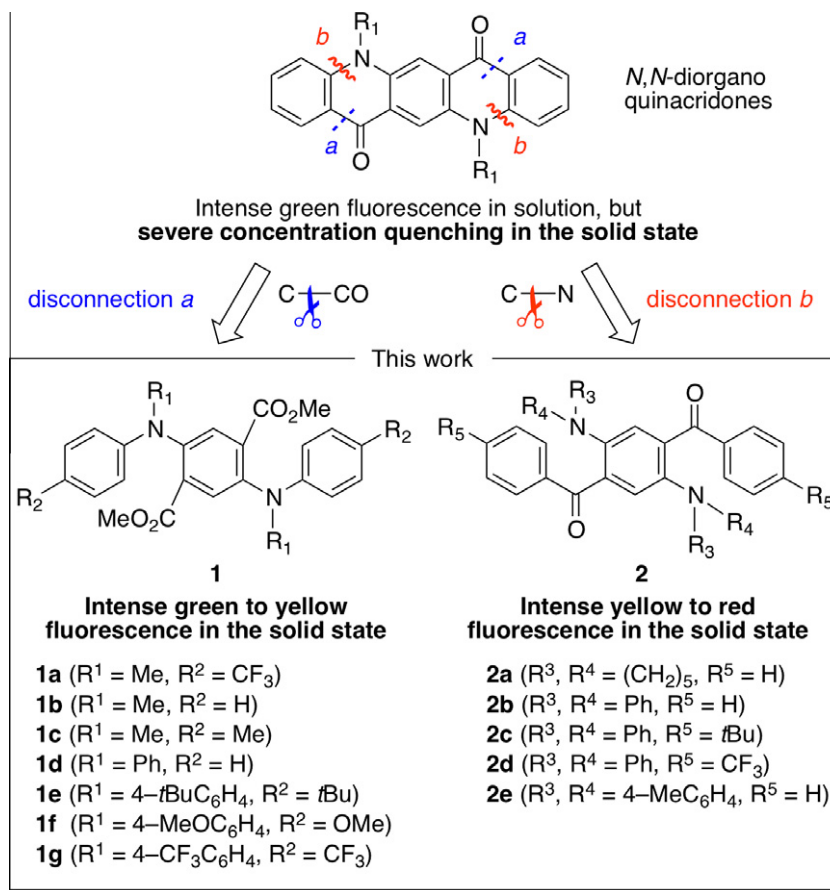
^{*} Corresponding author. Tel.: +81 75 383 2444; fax: +81 75 383 2445.

E-mail address: m.shimizu@hs2.ecs.kyoto-u.ac.jp (M. Shimizu).

[†] Present address: Research & Development Initiative, Chuo University, 1-13-27, Kasuga, Bunkyo-ku, Tokyo 112-8551, Japan.

In this communication, we present a new guiding principle for the design of organic fluorophores that emit visible light in the solid-state with high efficiency; this principle involves double disconnection of *N,N*-diorganoquinacridones, which show intense green fluorescence in solution but undergo severe luminescence quenching in the solid-state (Scheme 1). The approach allows the development of dimethyl 2,5-bis(diorganoamino)terephthalates **1** and 1,4-diaroyl-2,5-bis(diorganoamino)benzenes **2**, which exhibit efficient solid-state fluorescence in the green to yellow and yellow to red spectral regions, respectively. The high efficiency of the solid-state emissions is attributed to the nonplanar molecular frameworks and the intramolecular charge-transfer (CT) character of the S_1 states. Moreover, it is notable that **2** are fluorescent although benzophenone and its derivatives are generally nonfluorescent due to rapid intersystem crossing (ISC) from the S_1 state to the T_1 state.

Organic chromophores that consist of planar and rigid π -conjugated systems generally exhibit luminescence with high efficiency in solution, where the chromophores are sufficiently isolated for them not to interact electronically with one another. The planarity of the molecular framework enhances π -conjugation, and the rigidity of the skeleton is beneficial in the restriction of both the stretching and twisting motions of each bond, which can result in radiationless deactivation of the excited states. However, planar polycyclic chromophores normally show a strong tendency to aggregate in the solid-state, with a π - π stacked geometry that causes severe luminescence quenching. Typical examples are *N,N*-diorganoquinacridones, which exhibit intense green-emissions in dilute solution, but are non or weakly-emissive in



Scheme 1. Molecular design of highly emissive organic solids on the basis of planarity breaking of *N,N*-diorganoquinacridones.

the solid-state and even in concentrated solution.⁶ For example, the photoluminescence quantum yields of *N,N*-dibutyl-2,9-difluoroquinacridone were reportedly 0.97 in THF (1.0×10^{-6} M) and 0.0019 in the microcrystals.^{6a} They are, therefore, used as dopants in OLED devices.⁷

We have recently demonstrated that 1,4-bis(alkenyl)-2,5-dipiperidinobenzenes are highly emissive fluorophores in the solid-state.⁸ Through an investigation of their structural characteristics and photophysical properties, we concluded that breaking the high planarity of *N,N*-diorganoquinacridones by disconnection of the bonds linked to the outer benzene rings, while retaining the electronic structure consisting of a 1,4-diamino-2,5-dicarbonyl functionality on the central benzene core, would provide new chromophores exhibiting highly efficient visible-light fluorescence in the solid-state if the two sets of *ortho*-linkages of the diorganoamino and carbonyl groups could induce a twisted conformation suitable for suppression of dense stacking in the ground state and a large Stokes shift leading to inhibition of Förster-type energy transfer from the excited state.

Based on this idea, there are two options for the disconnection (Scheme 1); one is cleavage of the C–CO bonds (indicated by dotted blue lines (a)), and the other involves fission of the C–N bonds (indicated by wavy red lines (b)). We initially designed dimethyl 2,5-bis(arylamino)terephthalates **1** as disconnection a, and prepared them in good to high yields from dimethyl 2,5-dibromoterephthalate and anilines by Pd-catalyzed amination or commercially available dimethyl 2,5-dioxocyclohexane-1,4-dicarboxylate via three steps (see the Supplementary data for details).⁹

Single crystals of **1b** suitable for X-ray diffraction analysis were obtained by recrystallization from dichloromethane/hexane

solution.⁹ As shown in Figure 1, the phenyl and methyl groups of the amino moiety as well as the methoxy groups are positioned largely out of the central benzene plane (C2–C3–N1–C4 = 50.28°; C3–C2–C1–O1 = 40.45°) and the distances between the centroids of the central benzene rings in two adjacent molecules in the crystal lattice are over 6 Å; there is no intermolecular aromatic interaction like π – π stacking to cause emission quenching. The molecular and crystal structures of **1d** also show similar distorted molecular conformations and the absence of π – π stacking.⁹

Absorption and fluorescence spectra of **1d** in toluene are shown in Figure 2 as representative examples.⁹ The absorption maxima appeared at 343 nm ($\epsilon = 16800$) and 415 nm ($\epsilon = 4300$), and green fluorescence was observed with an emission maximum at 547 nm and a quantum yield of 0.40. Thus, there was no overlap of the absorption and fluorescence spectra, suggesting that photo-excitation induced the large structural change in **1d**. When a solvent was changed from toluene to dichloromethane, the fluorescence spectra red-shifted ($\lambda_{\text{em}} = 564$ nm, $\phi_{\text{f}} = 0.11$) as shown in Figure 2.⁹

The HOMO, LUMO, and LUMO+1 of **1d** obtained by density functional theory (DFT) calculations at the B3LYP/6-31G(d) level are depicted in Figure 3.¹⁰ The HOMO is developed over the Ph₂N–benzene–NPh₂ framework, while the MeO₂C–benzene–CO₂Me unit contributes to the LUMO. Time-dependent DFT calculations reveal that the lowest energy transition is governed mainly by the HOMO–LUMO transition.¹¹ Thus, the absorption band at 415 nm can be ascribed to an intramolecular CT transition, which is consistent with the large Stokes shift and the solvatochromism.

The photoluminescence properties of **1** in the crystalline and powder states are summarized in Table 1, together with those in toluene (the spectra are shown in Supplementary data). Upon photo-irradiation, solid **1** exhibited intense solid-state fluorescence

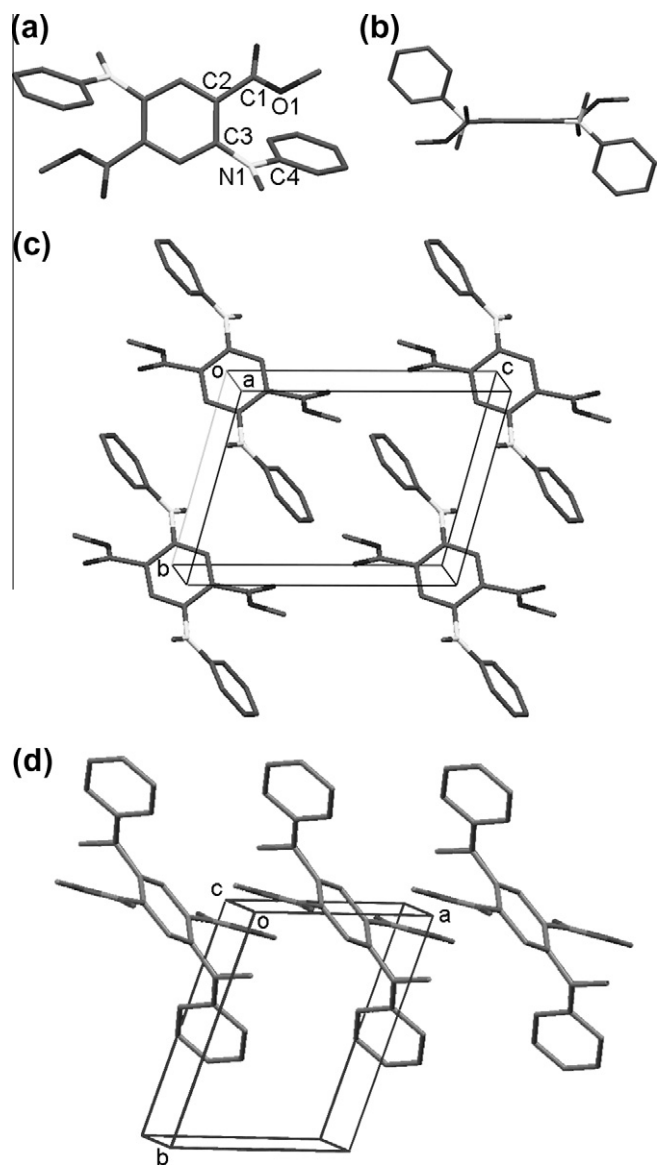


Figure 1. Molecular and crystal structures of **1b**: space group P-1 (triclinic), $a = 6.0995(13)$, $b = 8.5112(19)$, $c = 11.134(2)$, $\alpha = 95.713(4)^\circ$, $\beta = 104.354(4)^\circ$, $\gamma = 107.081(4)^\circ$. Hydrogens are omitted for clarity. (a) top view, (b) side view, (c) packing view from a axis, and (d) packing view from c axis.

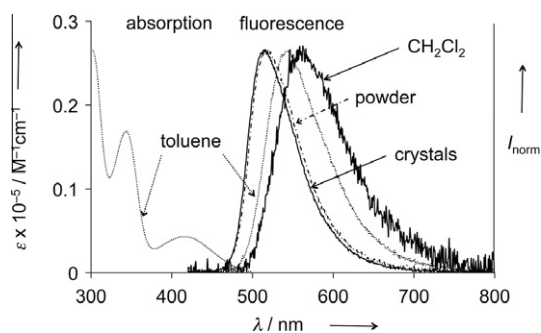


Figure 2. Absorption and fluorescence spectra of **1d**.

ranging from green to yellow, with good to high quantum yields ($\phi_f = 0.32$ – 0.76). The fluorescence spectra of solid **1d** are shown in Figure 2.⁹ Some photographs of the irradiated samples are shown in Figure 4. There is no big difference between the emission

maxima in the crystalline and powder states for each compound. In all cases, ϕ_f values in solution were much lower than those in the solid-state; **1** were found to exhibit aggregation-induced emission (AIE).¹² The serious nonradiative decay in solution is presumably attributable to the intramolecular free motion of the amino and methoxycarbonyl moieties. Diethyl bis(4-trifluoromethylphenylamino)terephthalate and diethyl bis[3,5-bis(trifluoromethyl)phenylamino]terephthalate are reported to display unique thermal stimuli-induced switching of solid-state fluorescence.¹³ Since the quantum yields of the ArNH-substituted terephthalates in the solid-state ranged from 0.066 to 0.410, it is apparent that the presence of the second carbonaceous substituents on the nitrogens of **1** is essential for attaining high solid-state quantum yields in molecular design based on 2,5-diaminoterephthalate frameworks.¹⁴

Diaminodiaroylbenzenes **2**, designed as disconnection **b** (Scheme 1), were synthesized as colored solids from 2,5-dibromoterephthaloyl dichloride via three steps (Figure 5a–h, the upper photographs).⁹ During purification and isolation, we observed that the colors of the isolated solids **2b** and **2e** were very sensitive to the preparative history of each solid sample. Recrystallization of **2b** from THF/MeOH solution and slow evaporation (220 hPa, 40 °C) of a THF solution gave yellow microcrystals and powder (Fig. 5c,d), respectively; quick evaporation (60 hPa, 40 °C) afforded a red powder (Fig. 5e). DSC analysis of **2b** in red powder showed an exothermic phase-transition peak at 127 °C.⁹ When the red powder was heated at 130 °C, it changed color to yellow. Recrystallization of **2e** from THF/MeOH solution provided red microcrystals (Fig. 5f), and quick evaporation of a THF solution left a mixture of orange and red powders. Interestingly, all of the red powder in the mixture turned orange (Fig. 5g) upon heating the mixture at 100 °C.⁹ In turn, the resulting orange powder gradually and completely turned red (Fig. 5h) when the powder was exposed to dichloromethane vapor for 24 h.¹⁵ The color-changing process was found to be reversible. These observations indicate that the photophysical properties of **2b** and **2e** in the solid-state are very sensitive to subtle differences in morphology.

With this morphology-sensitive behavior of **2** in mind, we measured the photoluminescence of the crystals and powders. The results are summarized in Table 2, along with the results obtained from measurements in toluene. All of the prepared solid samples emitted brilliantly visible light ranging from yellow to deep red (Fig. 5a–h, the lower photographs). Comparison of the solid-state emissions with those in solution confirms that **2** are also AIE-active chromophores. There was no overlap of the absorption and emission spectra of **2**; in other words, large Stokes shifts were observed, as illustrated by the example of **2b** in Figure 6. Changing a solvent from toluene to dichloromethane induced a

Table 1
Photoluminescence data of **1**

Entry	1	λ_{em}^a (nm) (ϕ_f) ^b		
		Microcrystals ^c	Powder ^d	Solution ^e
1	1a	523 (0.47)	527 (0.32)	514 (0.15)
2	1b	539 (0.64)	544 (0.60)	544 (0.03)
3	1c	553 (0.47)	549 (0.43)	— ^f
4	1d	519 (0.44)	516 (0.71)	547 (0.40)
5	1e	572 (0.67)	565 (0.76)	556 (0.18)
6	1f	571 (0.60)	568 (0.63)	— ^f
7	1g	504 (0.76)	508 (0.72)	499 (0.54)

^a Emission maxima upon photo-irradiation ($\lambda_{ex} = 400$ nm).

^b Absolute quantum yield determined with a calibrated integrating sphere system.

^c Prepared by recrystallization from dichloromethane/hexane.

^d Prepared by evaporation (600 hPa, 40 °C) of CH_2Cl_2 solution.

^e 1×10^{-5} M in toluene.

^f No fluorescence was observed.

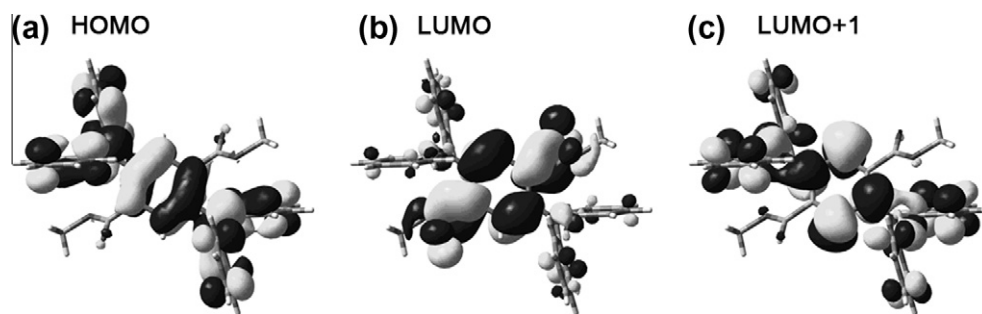


Figure 3. HOMO (a), LUMO (b), and LUMO+1 (c) diagrams of **1d**.

red-shift of the fluorescence spectra as observed with **1** (see the Supplementary data for details).⁹ X-ray single crystal analysis of **2a** revealed that the piperidyl and benzoyl groups were largely out of the central benzene plane.⁹ DFT calculations indicate that the photoluminescence is also governed by intramolecular CT transitions (Fig. 7).¹⁰ The emissions appeared in a longer wavelength region than those of **1**; this can be ascribed to the enhanced intramolecular CT character of the transitions as a result of the stronger electron-withdrawing effects of aryl moieties compared with those of methoxycarbonyl groups. Since red-emissive organic fluorophores in the neat solid-state generally have a strong tendency to cause aggregation, which results in severe concentration quenching, it is a formidable challenge to attain quantum yields exceeding 0.3 with regard to red emissions from neat organic solids.¹⁶ It is, therefore, noteworthy that **2d** and **2e** in crystals exhibit red emission at 640 and 650 nm with excellent quantum yields of 0.33 and 0.47, respectively.

It should be noted that the luminescence from **2** originates in radiative decay of the S_1 state, that is, fluorescence; this is confirmed by lifetime measurements; τ **2a**, crystal) = 15.2 ns and

5.9 ns; τ **2a**, powder) = 8.1 ns; τ **2b**, crystal) = 22.5 ns; τ **2b**, powder) = 10.3 ns and 4.7 ns.¹⁷ Generally, diaryl ketones in which the orbital configuration of the S_1 state is assigned to $n-\pi^*$ transitions of the ketone carbonyl group are almost nonfluorescent ($\phi_f = \sim 0.01-0.0001$) because ISC from the S_1 state to the T_1 state is much faster than the relatively slow radiative decay.¹⁸ For example, benzophenone exhibits no fluorescence in solution at room temperature and shows phosphorescence at low temperatures in a frozen solvent due to highly efficient ISC ($\phi_{ISC} = 1.0$).¹⁹ Room-temperature phosphorescence from crystals of benzophenone and its derivatives have also been demonstrated very recently.²⁰ Compared with these features of phosphorescence emissions from diaryl ketones, the observed efficient fluorescence from **2**, which possesses two diaryl ketone moieties, clearly implies that the intramolecular CT transitions induced by the amino groups substituted at the *ortho*-positions mainly govern the electronic structure of the S_1 state in favor of the $n-\pi^*$ transitions of the ketone carbonyls. This is consistent with nearly no distribution of the HOMO on the carbonyl oxygen and significant contribution of the amino groups to the HOMO (Fig. 7).

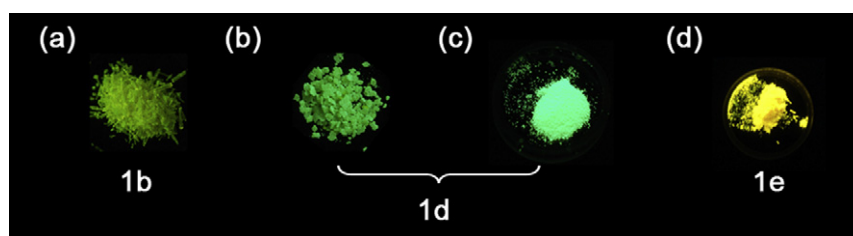


Figure 4. Photoluminescence images of **1**: (a) crystals of **1b**, (b) crystals of **1d**, (c) powder of **1d**, and (d) powder of **1e**.

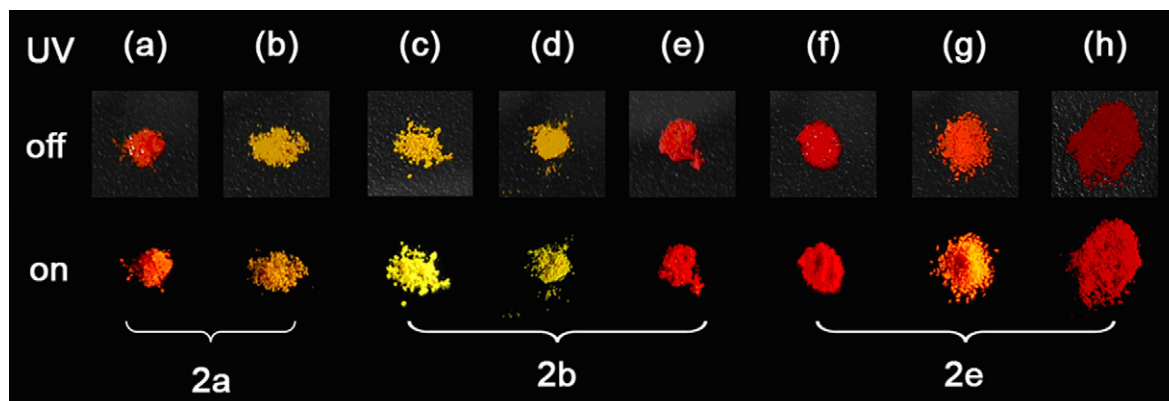
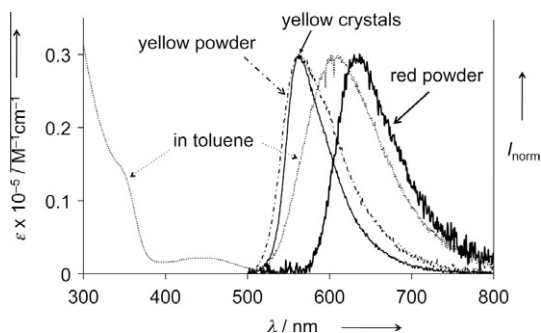


Figure 5. Optical and fluorescence images of **2**: (a) crystals of **2a**, (b) powder of **2a**; (c) crystals of **2b**; (d) yellow powder of **2b**; (e) red powder of **2b**; (f) crystals of **2e**; (g) orange powder of **2e**; and (h) red powder of **2e** under natural light (the upper photograph of each entry) and a UV lamp (the lower photograph of each entry).

Table 2
Photoluminescence data of **2**^a

Entry	2	Color and shape	λ_{em}^b (nm)	ϕ_f^c
1	2a	Orange crystals ^d	608	0.38
2		Orange powder ^e	588	0.14
3		(In toluene) ^f	— ^g	— ^g
4	2b	Yellow crystals ^d	562	0.61
5		Yellow powder ^h	565	0.35
6		Red powder ^e	637	0.22
7		(In toluene) ^f	602	0.20
8	2c	Orange crystals ^d	614	0.60
9		Orange powder ^e	610	0.44
10		(In toluene) ^f	603	0.23
11	2d	Red crystals ^d	640	0.33
12		Red powder ^e	640	0.18
13		(In toluene) ^f	633	0.14
14	2e	Red crystals ^d	650	0.47
15		Orange powder ⁱ	610	0.30
16		Red powder ^j	657	0.20
17		(In toluene) ^f	623	0.16

^a Irradiation was effected at 400 nm for **2a** and 450 nm for **2b–e**.^b Emission maxima.^c Absolute quantum yield determined with a calibrated integrating sphere system.^d Prepared by recrystallization from THF/MeOH solution.^e Prepared by evaporation (60 hPa, 40 °C) of THF solution.^f 2×10^{-5} M in toluene.^g No fluorescence was observed.^h Prepared by slow evaporation (220 hPa, 40 °C) of THF solution.ⁱ Prepared by evaporation (60 hPa, 40 °C) of THF solution followed by heating at 100 °C.^j Prepared by evaporation (60 hPa, 40 °C) of THF solution followed by heating at 100 °C, and then exposure to a vapor of dichloromethane for 24 h.**Figure 6.** Absorption spectra of **2b** in toluene and fluorescence spectra of **2b** in toluene, as crystals, and as a powder.

In summary, we have demonstrated that dimethyl 2,5-bis(diorganoamino)terephthalates and 1,4-diaroyl-2,5-bis(diorganoamino)benzenes in the solid-state exhibit intense green to yellow and yellow to red fluorescence, respectively, with good to high quantum yields.²¹ In particular, it is remarkable that an excellent

quantum yield of solid-state red fluorescence is attained with 1,4-dibenzoyle-2,5-bis(4-methylphenyl)benzene ($\phi_f = 0.47$ with an emission maximum of 650 nm). The molecular design of these new solid fluorophores originates in the idea of planarity breaking of *N,N*-diorganoquinacridones, and the success of the design is now prompting us to apply this molecular design concept to other types of planar dopant emitters, such as coumarins, in order to extend the validity of the design principle. Furthermore, we have found that 1,4-diaroyl-2,5-bis(diorganoamino)benzenes constitute a new class of polymorphic solids that exhibit morphology-sensitive luminescence. These findings make 2,5-bis(diorganoamino)-1,4-diaroylbenzenes potentially attractive as organic emitting materials, not only for OLEDs, but also for sensing and switching devices that utilize solid-state luminescence as an output.²² Further studies on these polymorphic structures and their relationship with photophysical properties are in progress.

Acknowledgments

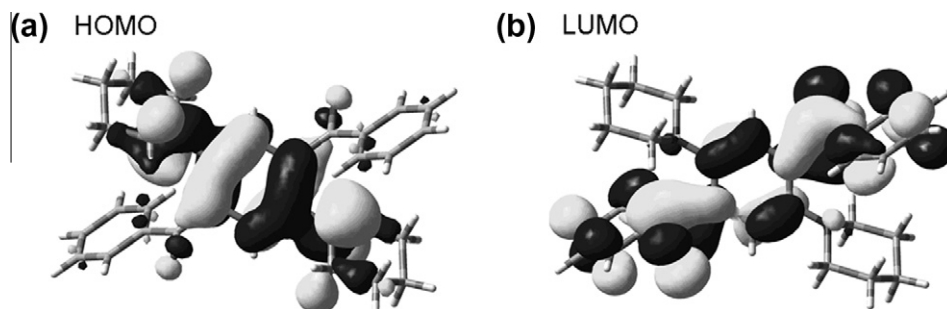
This work was supported by Grants-in-Aid for Creative Scientific Research, No. 16GS0209, and Scientific Research, No. 22350081, from the Ministry of Education, Culture, Sports, Science and Technology, Japan. The authors thank Mr. Hirohiko Watanabe, Hamamatsu Photonics K.K. for measurement of luminescence lifetime.

Supplementary data

Supplementary data associated with this article can be found, in the online version, at doi:10.1016/j.tetlet.2011.05.087.

References and notes

- (a) *Highly Efficient OLEDs with Phosphorescent Materials*; Yersin, H., Ed.; Wiley-VCH: Weinheim, 2008; (b) *Organic Light-Emitting Devices. Synthesis, Properties and Applications*; Müllen, K., Scherf, U., Eds.; Wiley-VCH: Weinheim, 2006; (c) Friend, R. H.; Gymer, R. W.; Holmes, A. B.; Burroughes, J. H.; Marks, R. N.; Taliani, C.; Bradley, D. D. C.; Dos Santos, D. A.; Brédas, J. L.; Lögdlund, M.; Salaneck, W. R. *Nature* **1999**, *397*, 121–128.
- (a) Zaumseil, J.; Siringhaus, H. *Chem. Rev.* **2007**, *107*, 1296–1323; (b) Ciccoira, F.; Santato, C. *Adv. Funct. Mater.* **2007**, *17*, 3421–3434.
- (a) Samuel, I. D. W.; Turnbull, G. A. *Mater. Today* **2004**, *7*, 28–35; (b) Scherf, U.; Riechel, S.; Lemmer, U.; Mahrt, R. F. *Curr. Opin. Solid State Mater. Sci.* **2001**, *5*, 143–154; (c) McGehee, M. D.; Heeger, A. J. *Adv. Mater.* **2000**, *12*, 1655–1668; (d) Kranzelbinder, G.; Leising, G. *Rep. Prog. Phys.* **2000**, *63*, 729–762; (e) Tessler, N. *Adv. Mater.* **1999**, *11*, 363–370; (f) Kozlov, V. G.; Forrest, S. R. *Curr. Opin. Solid State Mater. Sci.* **1999**, *4*, 203–208; (g) Dodabalapur, A.; Chandross, E. A.; Berggren, M.; Slusher, R. E. *Science* **1997**, *277*, 1787–1788.
- Reviews on fluorescent sensors: (a) Thomas, S. W.; Joly, G. D.; Swager, T. M. *Chem. Rev.* **2007**, *107*, 1339–1386; (b) Carol, P.; Sreejith, S.; Ajayaghosh, A. *Chem. Asian J.* **2007**, *2*, 338–348; (c) Basabe-Desmonts, L.; Reinhoudt, D. N.; Crego-Calama, M. *Chem. Soc. Rev.* **2007**, *36*, 993–1017; (d) Wolfbeis, O. S. *J. Mater. Chem.* **2005**, *15*, 2657–2669; (e) Callan, J. F.; De Silva, A. P.; Magri, D. C. *Tetrahedron* **2005**, *61*, 8551–8588; (f) Martínez-Manez, R.; Sancenón, F. *Chem. Rev.* **2003**, *103*, 4419–4476; (g) De Silva, A. P.; Gunaratne, H. Q. N.; Gunlaugsson, T.; Huxley, A. J. M.; McCoy, C. P.; Rademacher, J. T.; Rice, T. E. *Chem. Rev.* **1997**, *97*, 1515–1566; Selected examples of solid-state fluorescent sensors: (h) Esser, B.; Swager, T. M. *Angew. Chem., Int. Ed.* **2010**, *49*, 8872–8875;

**Figure 7.** HOMO (a) and LUMO (b) diagrams of **2a**.

- (i) Sreejith, S.; Divya, K. P.; Ajayaghosh, A. *Chem. Commun.* **2008**, 2903–2905; (j) Dale, T. J.; Rebek, J. *J. Am. Chem. Soc.* **2006**, *128*, 4500–4501; (k) Zhang, S. W.; Swager, T. M. *J. Am. Chem. Soc.* **2003**, *125*, 3420–3421; (l) Yang, J. S.; Swager, T. M. *J. Am. Chem. Soc.* **1998**, *120*, 11864–11873; (m) Yang, J. S.; Swager, T. M. *J. Am. Chem. Soc.* **1998**, *120*, 5321–5322.
5. Review on small organic molecules exhibiting highly efficient solid-state fluorescence: (a) Shimizu, M.; Hiyama, T. *Chem. Asian J.* **2010**, *5*, 1516–1531; Design and development of efficiently luminescent organic gels: (b) Babu, S. S.; Kartha, K. K.; Ajayaghosh, A. *J. Phys. Chem. Lett.* **2010**, *1*, 3413–3424; (c) Babu, S. S.; Praveen, V. K.; Prasanthkumar, S.; Ajayaghosh, A. *Chem. Eur. J.* **2008**, *14*, 9577–9584; (d) Ajayaghosh, A.; Praveen, V. K.; Srinivasan, S.; Varghese, R. *Adv. Mater.* **2007**, *19*, 411–415; (e) An, B.-K.; Lee, D.-S.; Lee, J.-S.; Park, Y.-S.; Song, H.-S.; Park, S. Y. *J. Am. Chem. Soc.* **2004**, *126*, 10232–10233.
6. (a) Zhao, Y.; Mu, X.; Bao, C.; Fan, Y.; Zhang, J.; Wang, Y. *Langmuir* **2009**, *25*, 3264–3270; (b) Fan, Y.; Zhao, Y.; Ye, L.; Li, B.; Yang, G.; Wang, Y. *Cryst. Growth Des.* **2009**, *9*, 1421–1430; (c) Wang, J.; Zhao, Y.; Zhang, J.; Yang, B.; Wang, Y.; Zhang, D.; You, H.; Ma, D. *J. Phys. Chem. C* **2007**, *111*, 9177–9183; (d) Mizuguchi, J.; Senju, T. *J. Phys. Chem. B* **2006**, *110*, 19154–19161; (e) Ye, K.; Wang, J.; Sun, H.; Liu, Y.; Mu, Z.; Li, F.; Jiang, S.; Zhang, H.; Wang, Y.; Che, C. M. *J. Phys. Chem. B* **2005**, *109*, 8008–8016.
7. *N,N*-Diphenylquinacridone: (a) Shi, J.; Tang, C. W. *Appl. Phys. Lett.* **1997**, *70*, 1665–1667; *N,N*-Dibutylquinacridone: (b) Murata, H.; Merritt, C. D.; Inada, H.; Shirota, Y.; Kafafi, Z. H. *Appl. Phys. Lett.* **1999**, *75*, 3252–3254. *N,N*-Diethylquinacridone: (c) Ref. [6e]; *N,N*-Dimethylquinacridone: (d) Dobbertin, T.; Werner, O.; Meyer, J.; Kammoun, A.; Schneider, D.; Riedl, T.; Becker, E.; Johannes, H. H.; Kowalsky, W. *Appl. Phys. Lett.* **2003**, *83*, 5071–5073.
8. Shimizu, M.; Takeda, Y.; Higashi, M.; Hiyama, T. *Angew. Chem., Int. Ed.* **2009**, *48*, 3653–3656.
9. Supplementary data includes preparation, characterization data, and data on photophysical properties of **1** and **2**. Crystallographic data for **1b**, **1d**, and **2a** (CCDC–801000, –801001, and –801002), and DSC charts of **2b** and **2e** in powder are also shown in Supplementary data. Although compound **1d** was reportedly prepared as an intermediate in the preparation of poly[(diaminophenylene)vinylene]s, no photophysical properties and crystal structure of **1d** were examined Shi, J.; Zheng, S. *Macromolecules* **2001**, *34*, 6571–6576.
10. DFT calculations of **1d** and **2a** at the B3LYP/6-31G(d) level were carried out using the crystal structures by the Gaussian 03 package (Revision E.01, M. J. Frisch et al., Gaussian, Inc., Wallingford CT, 2004). For details, see Supplementary data.
11. The higher transition can be assigned to the HOMO–LUMO+1 transition (π – π^* transition).
12. (a) Luo, J.; Xie, Z.; Lam, J. W. Y.; Cheng, L.; Chen, H.; Qiu, C.; Hoi Sing, K.; Zhan, X.; Liu, Y.; Zhu, D.; Tang, B. Z. *Chem. Commun.* **2001**, 1740–1741; (b) Hong, Y.; Lam, J. W. Y.; Tang, B. Z. *Chem. Commun.* **2009**, 4332–4353; (c) Liu, J.; Lam, J. W. Y.; Tang, B. Z. *J. Inorg. Organomet. Polym. Mater.* **2009**, *19*, 249–285. and references cited therein.
13. Zhao, Y.; Gao, H.; Fan, Y.; Zhou, T.; Su, Z.; Liu, Y.; Wang, Y. *Adv. Mater.* **2009**, *21*, 3165–3169.
14. Fluorescence quantum yields of 2,5-bis(arylamino)terephthalates in solution were reportedly to range from 0.013 to 0.23 Zhang, Y.; Starynowicz, P.; Christoffers, J. *Eur. J. Org. Chem.* **2008**, 3488–3495.
15. We confirmed that no detectable dichloromethane was present in the red powder of **2e** by ^1H NMR, indicating that the color change from orange to red did not result from the formation of inclusion/co-ordination complexes of **2e** and dichloromethane. Examples of solvent vapor-induced color/luminescence change of chromophores in the solid-state: (a) Ooyama, Y.; Kagawa, Y.; Fukuoka, H.; Ito, G.; Harima, Y. *Eur. J. Org. Chem.* **2009**, 5321–5326; (b) Dong, Y.; Lam, J. W. Y.; Qin, A.; Li, Z.; Sun, J.; Sung, H. H. Y.; Williams, I. D.; Tang, B. Z. *Chem. Commun.* **2007**, 40–42; (c) Fukushima, T.; Takachi, K.; Tsuchihara, K. *Macromolecules* **2006**, *39*, 3103–3105; (d) Ohshita, J.; Lee, K. H.; Hashimoto, M.; Kunugi, Y.; Harima, Y.; Yamashita, K.; Kunai, A. *Org. Lett.* **2002**, *4*, 1891–1894; (e) Rakow, N. A.; Suslick, K. S. *Nature* **2000**, *406*, 710–713.
16. (a) Chen, C. T. *Chem. Mater.* **2004**, *16*, 4389–4400; (b) Ref. [5]; (c) Wakamiya, A.; Mori, K.; Yamaguchi, S. *Angew. Chem., Int. Ed.* **2007**, *46*, 4273–4276; (d) Matsui, M.; Ikeda, R.; Kubota, Y.; Funabiki, K. *Tetrahedron Lett.* **2009**, *50*, 5047–5049.
17. Lifetimes of photoluminescence were measured with Quantaaurus-Tau (Hamamatsu Photonics K.K.).
18. Turro, N. J. *Modern Molecular Photochemistry*; University Science Books: Sausalito, 1978. chapter 5.
19. Lamola, A. A.; Hammond, G. S. *J. Chem. Phys.* **1965**, *43*, 2129–2135.
20. Yuan, W. Z.; Shen, X. Y.; Zhao, H.; Lam, J. W. Y.; Tang, L.; Lu, P.; Wang, C.; Liu, Y.; Wang, Z.; Zheng, Q.; Sun, J. Z.; Ma, Y.; Tang, B. Z. *J. Phys. Chem. C* **2010**, *114*, 6090–6099.
21. We preliminarily confirmed that UV irradiation of **1b**, **1d**, **2a**, and **2b** in the solid-state with a 400 W high-pressure mercury lamp at room temperature for 6 h resulted in no change of the fluorescence spectra and quantum yields.
22. (a) Mutai, T.; Tomoda, H.; Ohkawa, T.; Yabe, Y.; Araki, K. *Angew. Chem., Int. Ed.* **2008**, *47*, 9522–9524; (b) Quartapelle Procopio, E.; Mauro, M.; Panigati, M.; Donghi, D.; Mercandelli, P.; Sironi, A.; D'Alfonso, G.; De Cola, L. *J. Am. Chem. Soc.* **2010**, *132*, 14397–14399; (c) Anthony, S. P.; Draper, S. M. *J. Phys. Chem. C* **2010**, *114*, 11708–11716; (d) Sagara, Y.; Kato, T. *Nature Chem.* **2009**, *1*, 605–610.